AD-A088 532 WISCONSIN UNIV-MADISON DEPT OF CHEMISTRY F/G 7/4
LUMINESCENT TELLURIUM-DOPED CADMIUM SULFIDE ELECTRODES AS PROBE--ETC(U)
AUG 80 A B ELLIS, B R KARAS, H H STRECKERT N00014-78-C-0633
UNCLASSIFIED TR-3 NL

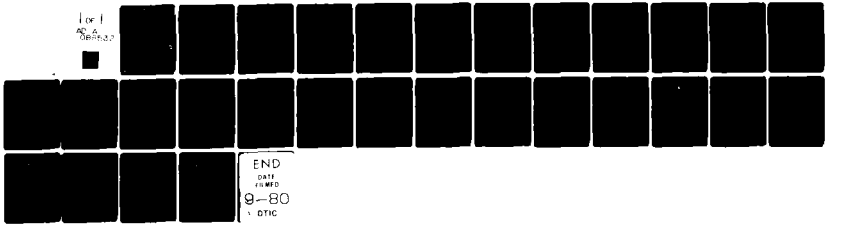

END
DATE FILMED
9-80
DTIC

LEVEL II

12

OFFICE OF NAVAL RESEARCH

15 Contract No. N00014-78-C-0633

Task No. NR 051-690

9 TECHNICAL REPORT NO. 3

6

Luminescent Tellurium-Doped Cadmium Sulfide Electrodes as Probes of Semiconductor Excited-State Deactivation Processes in Photoelectrochemical Cells.

by

14

Arthur B. Ellis*, Bradley R. Karas and Holger H. Streckert

Prepared for publication

in

Discussions of the Faraday Society No. 70
(Photoelectrochemistry)

Department of Chemistry
University of Wisconsin
Madison, Wisconsin 53706

11 12 August 1980 12

Approved for Public Release: Distribution Unlimited

*To whom all correspondence should be addressed.

Unclassified

SECURITY CLASSIFICATION OF THIS PAGE (When Data Entered)

REPORT DOCUMENTATION PAGE	READ INSTRUCTIONS BEFORE COMPLETING FORM
1. REPORT NUMBER: Technical Report No. 3 / 2. GOVT ACCESSION NO.: AD-A068 532	3. RECIPIENT'S CATALOG NUMBER
4. TITLE (and Subtitle): Luminescent Tellurium-Doped Cadmium Sulfide Electrodes as Probes of Semiconductor Excited-State Deactivation Processes in Photoelectrochemical Cells.	5. TYPE OF REPORT & PERIOD COVERED
	6. PERFORMING ORG. REPORT NUMBER
7. AUTHOR(s): Arthur B. Ellis, Bradley R. Karas and Holger H. Streckert	8. CONTRACT OR GRANT NUMBER(s): N00014-C-78-0633
9. PERFORMING ORGANIZATION NAME AND ADDRESS: Department of Chemistry, University of Wisconsin, Madison, Wisconsin 53706	10. PROGRAM ELEMENT, PROJECT, TASK AREA & WORK UNIT NUMBERS: NR 051-690
11. CONTROLLING OFFICE NAME AND ADDRESS: Office of Naval Research/Chemistry Program Arlington, Virginia 22217	12. REPORT DATE: August 12, 1980
	13. NUMBER OF PAGES: 28
14. MONITORING AGENCY NAME & ADDRESS(if different from Controlling Office)	15. SECURITY CLASS. (of this report): Unclassified
	15a. DECLASSIFICATION/DOWNGRADING SCHEDULE

16. DISTRIBUTION STATEMENT (of this Report)

Approved for Public Release: *Distribution Unlimited*

17. DISTRIBUTION STATEMENT (of the abstract entered in Block 20, if different from Report)

18. SUPPLEMENTARY NOTES

Prepared for publication in Discussions of the Faraday Society, No. 70 (Photoelectrochemistry)

19. KEY WORDS (Continue on reverse side if necessary and identify by block number)

photoelectrochemistry; luminescence

20. ABSTRACT (Continue on reverse side if necessary and identify by block number)

Correlations between quantum efficiencies for photocurrent ($\phi_{(e)}$), emission (ϕ_r), and nonradiative recombination ($\phi_{(nr)}$) are discussed with reference to data from single-crystal, n-type, 100 and 1000 ppm CdS:Te-based photoelectrochemical cells (PECs) employing aqueous sulfide electrolyte. These materials emit while they serve as PEC electrodes. The assumption that the proportionality of $\phi_{(r)}$ to $\phi_{(nr)}$ is unaffected by potential leads to

DD FORM 1 JAN 73 1473 EDITION OF 1 NOV 65 IS OBSOLETE S/N 0102-LF-014-6601

Unclassified

SECURITY CLASSIFICATION OF THIS PAGE (When Data Entered)

20. Abstract (continued)

a simple expression relating ϕ_x to ϕ_r for monochromatic excitation. Calculated and observed emission data are in reasonable agreement; sources of deviation are discussed. Polychromatic excitation is shown to yield photocurrent and emission intensity which is approximately a weighted average of the values obtained with the constituent monochromatic frequencies. Practical implications of the ϕ_x correlation with ϕ_r are described, as are related results from other PECs.

Abstract

Correlations between quantum efficiencies for photocurrent (ϕ_x), emission (ϕ_r), and nonradiative recombination (ϕ_{nr}) are discussed with reference to data from single-crystal, n-type, 100 and 1000 ppm CdS:Te-based photoelectrochemical cells (PECs) employing aqueous sulfide electrolyte. These materials emit while they serve as PEC electrodes. The assumption that the proportionality of ϕ_r to ϕ_{nr} is unaffected by potential leads to a simple expression relating ϕ_x to ϕ_r for monochromatic excitation. Calculated and observed emission data are in reasonable agreement; sources of deviation are discussed. Polychromatic excitation is shown to yield photocurrent and emission intensity which is approximately a weighted average of the values obtained with the constituent monochromatic frequencies. Practical implications of the ϕ_x correlation with ϕ_r are described, as are related results from other PECs.

Luminescence, traditionally used to characterize excited-state properties, has found only limited use thus far in photoelectrochemical cells (PECs). Early studies involving emissive semiconductor photoelectrodes have employed n- and p-type GaP[1,3], n-type ZnO[2,3], n-type CdS[3], and n- and p-type GaAs.[3,4] We have focussed our attention recently on n-type, tellurium-doped CdS (CdS:Te).[5-7] As the photoanode in PECs employing aqueous (poly)chalcogenide electrolytes, single-crystal,100 and 1000 ppm CdS:Te emit while effecting the oxidation of (poly)chalcogenide species.

Emission from CdS:Te is believed to involve intraband gap states which are introduced by the lattice substitution of Te for S; the band gap of CdS:Te is estimated to be about equal to that of undoped CdS (~2.4 eV;~515 nm).[8-12] Holes trapped at Te sites can coulombically bind an electron in or near the conduction band; the radiative collapse of this exciton leads to emission. The emissive spectral distribution (λ_{max} ~600 and 650 nm for 100 and 1000 ppm CdS:Te, respectively) was found to be unperturbed when the material was used as a photoelectrode in a PEC.[5-7] Importantly, the doped electrodes mimic the electro-optical properties of undoped CdS-based PECs.[7,13]

Photocurrent and emission represent competing excited-state deactivation processes. The semiconductor excited state consists of a photogenerated conduction band electron and valence band hole (e^- - h^+ pair). This e^- - h^+ pair can either separate to yield photocurrent or recombine in a radiative or nonradiative fashion.[14] Emission thus serves as a probe of the recombination process. In this paper we examine relationships between photocurrent and emissive quantum efficiencies. We demonstrate that the relationships which we find to exist for the CdS:Te-based PEC are consistently interpreted in terms of band bending, optical penetration depth, and the competitive nature of the excited-state decay processes.

EXPERIMENTAL

Plates of vapor-grown, single-crystal, 100 and 1000 ppm CdS:Te, ~5x5x1 mm and oriented with the 5x5 faces perpendicular to the c-axis, were purchased from Cleveland Crystals, Inc., Cleveland, Ohio. Resistivities were ~2 ohm-cm (four point probe method). Concentrations of Te are estimates based on starting quantities. Samples were etched with 1:10 (v/v) Br_2/MeOH prior to use. Electrode and electrolyte preparation as well as electrochemical and optical instrumentation have been described previously.[7]

Front-surface emissive properties were characterized by placing the PEC in the sample compartment of an emission spectrometer, as diagrammed in Fig. 1. The Coherent Radiation CR-12 Ar ion laser excitation source was used with multiline mirrors. This provided various combinations of excitation wavelengths in a single ~3 mm dia. beam. Monochromatic excitation was achieved by passing the multiline beam through an Oriel Model 7240 monochromator whose grating was blazed at 500 nm. Operation of the monochromator in zero order allowed for polychromatic excitation; the composition of the polychromatic beam was determined with the aid of a Bausch and Lomb 33-86-07 monochromator. Light intensities were adjusted with laser power and neutral density filters. In all experiments the laser beam was 10X expanded and masked to fill the electrode surface. Incident intensity measurements required removal of the PEC from the spectrometer sample compartment; after reconstruction of the PEC, the light intensity was reduced to give matching photocurrent and subsequently measured with a Tektronix J16 radiometer (J6502 probe head; flat response 450-950 nm).

RESULTS

The experimental setup pictured in Figure 1 can be used to obtain current-luminescence-voltage (iLV) curves as a function of excitation wavelength. Since the emissive spectral distribution is unaffected by either electrode potential or laser excitation wavelength,[7] emission intensity is readily monitored at a single wavelength, generally the emission band maximum.

In Figures 2-4 and 5-7 we present iLV curves for 100 and 1000 ppm CdS:Te-based PECs, respectively, employing transparent, aqueous, sulfide electrolyte. Although the data shown were obtained point-by-point with equilibration periods of ~20 seconds, similar curves were also observed with sweep rates up to 100 mV/s. All data were obtained with ~0.2-1.0 mW/cm^2 monochromatic or polychromatic laser excitation.

With regard to monochromatic excitation, there is a strong distinction between 514.5 nm and the shorter laser wavelengths. For comparable intensities 514.5 nm light (Fig. 2 and 5) generally yields substantially less photocurrent and greater emission intensity than is found with $\lambda \leq 500$ nm of which 488.0 nm excitation is illustrative (Fig. 3 and 6). A second recurrent feature is that despite its relatively large intensity, emission from 514.5 nm excitation is scarcely potential dependent (Fig. 2 and 5). Contrast this (Fig. 3 and 6) with the weaker emission intensity from 488.0 nm excitation which shows a marked potential dependence; in passing from -0.3 V vs. SCE to open circuit, the emission intensity increases by factors of almost 3 in Fig. 3 and 6.

Although only 488.0 nm iLV curves are pictured, our general observation has been that all Ar ion laser wavelengths from 457.9-501.7 nm give similar iLV properties.[5-7] We will subsequently refer to these as ultraband gap wavelengths, since their energies exceed the nominal band gap energy; absorptivities for these wavelengths are ~10^5 cm^{-1}.[8-12] Absorptivities for 514.5 nm excitation are in the 10^3-10^4 cm^{-1} range[8-12] so that designation of this line as band gap edge is more appropriate.

Polychromatic laser excitation was used for Fig. 4 and 7. Its power composition was roughly 35% 514.5 nm and 65% ultraband gap wavelengths, principally 488.0, 496.5, and 476.5 nm. As might be expected, the photocurrent and emission intensity from polychromatic excitation are bracketed by the values observed for pure 514.5 nm and ultraband gap excitation. In both the monochromatic and polychromatic

excitation experiments, the emission intensity (open circuit) and photocurrent (-0.3 V vs. SCE) varied linearly with light intensity over the relevant intensity regime.

DISCUSSION

MODEL

We will consider three routes for excited-state deactivation: separation of $e^- - h^+$ pairs to yield photocurrent, and recombination of $e^- - h^+$ pairs either radiatively or nonradiatively. The quantum efficiencies for these processes can be symbolized by ϕ_x, ϕ_r, and ϕ_{nr}, respectively. Treating these as the only decay routes yields the relationship

$$\phi_x + \phi_r + \phi_{nr} = 1 \qquad (1)$$

We have sought to determine how PEC experimental parameters influence the relative and absolute magnitudes of these quantum efficiencies. While absolute values for ϕ_x can be measured, we have had to content ourselves with relative ϕ_r measurements, owing to the experimental difficulties inherent in accounting for the spatial and spectral distribution of emitted light.[7,15] Measurements of ϕ_{nr} can be obtained with the technique of photothermal spectroscopy (PTS),[16-20] but we presently lack this information for the systems under scrutiny.

Simplification of the excited-state PEC description occurs at open circuit. In this case no $e^- - h^+$ pair separation can occur, making $\phi_x = 0$. The ratio of ϕ_r to ϕ_{nr} is easily shown to be dependent on excitation wavelength by comparing the emission intensities of Fig. 2 with Fig. 3 and Fig. 5 with Fig. 6 at open circuit. We have also previously shown this ratio to be temperature dependent at open circuit; ϕ_r decreases with increasing temperature.[21] The photoelectrode may thus be considered as having a characteristic open-circuit ratio of radiative to nonradiative recombination (ϕ_{r_o}/ϕ_{nr_o}), eq. (2), where k depends at least on

$$\phi_{nr_o} = k\phi_{r_o} \tag{2}$$

the excitation wavelength and temperature employed.

The effect of now bringing the PEC into circuit is to permit some fraction of $e^- - h^+$ pairs to separate rather than recombine. Values of ϕ_r and ϕ_{nr} can be potential dependent in the sense that different fractions of $e^- - h^+$ pairs are diverted from recombination, depending on the magnitude of the photocurrent, ϕ_x. Correlating ϕ_x with ϕ_r and ϕ_{nr} also involves knowing the relative extent to which radiatively and nonradiatively recombining $e^- - h^+$ pairs are prevented from recombining, i.e., their relative contributions to photocurrent. We will consider three simple schemes: photocurrent, ϕ_x, interconverts (1) exclusively with ϕ_{nr}; (2) exclusively with ϕ_r; (3) with both ϕ_r and ϕ_{nr} such that $\phi_{nr} = k\phi_r$ for any value of ϕ_x.

Scheme (1) predicts that emission intensity will be independent of potential. Although Fig. 2 and 5 appear in accord with this prediction, it is contradicted for ultraband gap excitation, as typified by Fig. 3 and 6. Scheme (2) is untenable because of the relative magnitudes of ϕ_r and ϕ_x. We have measured ϕ_r and ϕ_x to be $\sim 10^{-3}$ and 10^{-1}, respectively, for 514.5 nm excitation.[7] In passing from -0.3 V vs. SCE to open circuit in Fig. 2 and 5, Scheme (2) would predict a ~100-fold increase in emission intensity in contrast to the invariance observed. A similar argument can be made for ultraband gap excitation where ϕ_x is even larger. Scheme (3), although not perfect, is most compatible with our data. The ratio of emission intensities at any two potentials, 1 and 2, can be computed by combining eq. (1) and (2) to give eq. (3). For the case where the first potential is open circuit,

$$\frac{1 - \phi_{x_1}}{1 - \phi_{x_2}} = \frac{\phi_{r_1}}{\phi_{r_2}} \tag{3}$$

eq. (4) obtains. Table I consists of a compilation of ϕ_{r_o}/ϕ_r ratios as a

$$\frac{\phi_{r_o}}{\phi_r} = \frac{1}{1 - \phi_x} \tag{4}$$

function of ϕ_x.

We should point out that our treatment of ϕ_r and ϕ_x is not without precedent. Both GaP- and ZnO-based PECs have been examined in this regard.[1,2] The effects of optical penetration depth as well as carrier lifetime and diffusion length were considered in these studies which will be discussed below. More recently PTS has been utilized to establish relationships between ϕ_{nr} and ϕ_x.[16,18] In a very broad sense the competition among ϕ_r, ϕ_{nr}, and ϕ_x can be likened to a Stern-Volmer analysis[22] wherein photocurrent fills the role of the quencher in homogeneous molecular systems.

EXPERIMENTAL TESTS OF THE MODEL

The predictive value of eq. 4 for monochromatic excitation is analyzed with the aid of Table II which compares direct measurements of ϕ_x at -0.3 V vs. SCE with indirect determinations from ϕ_{r_o}/ϕ_r for each of the experiments in Fig. 2-7. Agreement is seen to be reasonably good. A more detailed comparison can be made by using each point of the iLV curve: After arbitrarily matching the calculated and observed open-circuit emission intensities, the measured ϕ_x at each potential was used to calculate (eq. 4) the corresponding emission intensity. Calculated intensities are indicated by the unfilled circles in Fig. 2, 3, 5, and 6.

Looking first at overall changes, band gap edge 514.5 nm excitation (Fig. 2 and 5, Table II) gave a maximum ϕ_x of ~0.1. From Table I we expect and observe little potential dependence of emission intensity. Low values of ϕ_x are consistent

with the comparatively large penetration depth of this wavelength; a substantial fraction of the incident light will be absorbed beyond the depletion region whose width is typically 10^{-4}-10^{-5} cm [14]. The lack of band bending beyond the depletion region favors e^- - h^+ pair recombination.

For the 488.0 nm excitation experiments maximum ϕ_x values are 0.49 and 0.74 for Fig. 3 and 6, respectively. The large ϕ_x values observed at these potentials and wavelengths are expected,since almost all of the light for ultraband gap wavelengths is absorbed within the depletion region. Between -0.3 V vs. SCE and open circuit, corresponding two- and four-fold increases in emission intensity are anticipated (Table I). There is some discrepancy between the calculated and observed emission data, although they generally differ by less than 20%.

The polychromatic excitation experiments of Fig. 4 and 7 were analyzed by two methods. Open circles in these figures correspond to calculations based on the measured value of ϕ_x and use of eq. 4. In essence this amounts to treating the exciting beam as monochromatic light. The inappropriateness of this treatment is apparent from the marked deviation of the calculated curves from those observed. We find, however, that the measured photocurrent and emission intensities from polychromatic excitation are in good agreement with a weighted average of the photocurrents and emission intensities of the constituent monochromatic lines. This can be seen by comparing Fig. 4 with Fig. 2 and 3,and Fig. 7 with Fig. 5 and 6; the 488.0 nm data is treated as representative of the ~56% and 71% ultraband gap composition of the polychromatic light in Fig. 4 and 7, respectively. Open triangles in Fig. 4 and 7 reveal that emission intensity calculated by this method is in much better agreement with the observed data. Implicit in the weighted-average procedure are the assumptions that the excitation wavelengths act independently of one another and that ϕ_x and ϕ_r are independent of intensity. The latter assumption was verified (vide supra).

Although Fig. 2-7 demonstrate reasonable agreement between calculated and observed emission intensity, we have seen iLV curves which cannot be accommodated by the simple scheme used thus far. For example, some iLV curves display "humps" wherein the luminescence-potential curve is characterized by maximum intensity at a potential other than open circuit. In this case there is a potential regime where both ϕ_x and ϕ_r are declining. We have also seen iLV curves where the photocurrent is constant and saturated over a potential range, but the emission intensity continues to decline in the direction of more positive potential. Here ϕ_x is constant but ϕ_r and ϕ_{nr} are changing with respect to one another, i.e., their proportionality constant is no longer independent of potential.

One possible explanation for these failures of the model is electroabsorption or potential-dependent absorptivity.[23] If electroabsorption were operative, it would mix the effects of optical penetration depth and band bending. Absorption of light in different regions of the electrode can give rise to different combinations of ϕ_r, ϕ_{nr}, and ϕ_x not only because of the differences in band bending, but also because the local environment in which $e^- - h^+$ pairs are formed may vary due to lattice defects, impurities, etc. Although we have not observed any direct evidence for electroabsorption effects, we have not been able to fully discount the possibility either.[7]

Properties of the semiconductor surface represent a second possible source of deviations from model predictions. Although luminescence from CdS:Te electrodes is primarily a volume effect, there is a contribution from holes trapped at Te sites near the surface. The magnitude of this contribution may be reflected in the decline in emission intensity with decreasing optical penetration depth; sites for nonradiative recombination are likely to be most prevalent near the surface. The filling and emptying of surface states with changes in potential could also influence ϕ_r when surface contributions to emission are not negligible.

Another possible surface effect arises in connection with our iLV curves which exhibit constant ϕ_x with declining ϕ_r values at positive potentials. This observation is reminiscent of data obtained in the ZnO-based PEC study where lower values of ϕ_r than expected were observed at positive potentials.[2] This was thought to be due to a deficiency in the electron concentration needed for recombination near the surface; in turn, this was ascribed to the considerable band bending present. In general we would predict that surface effects would be most significant with less penetrating ultraband gap wavelengths.

APPLICATIONS

Examination of relationships among ϕ_x, ϕ_{nr}, and ϕ_r has both theoretical and practical implications. In a theoretical sense we have tried to determine how the PEC experimental variables of excitation wavelength and potential influence the manner in which the semiconductor excited state partitions input optical energy. The assumption that the proportionality of ϕ_r to ϕ_{nr} is unaffected by potential leads to a simple expression (eq. 4) which fits much of our data for CdS:Te-based PECs. As described above, however, there are iLV curves which clearly violate the assumptions of the model.

Whether or not eq. 4 turns out to be a good prognosticator of relationships between ϕ_r and ϕ_x, it serves to illustrate the potential utility of such a correlation. For the systems at hand which appear to obey eq. 4, ϕ_x can be determined for monochromatic excitation simply by the use of a linearly-responsive light detector. That is, if the ratio between open-circuit and in-circuit emission intensity is known, then so, too, is ϕ_x at the in-circuit potential. The additional knowledge of the photocurrent permits calculation of the absorbed light intensity without having to correct measured light intensities for reflective losses, electrolyte absorption, etc.

One difficulty with the technique is that, as Table I indicates, it really only becomes sensitive when ϕ_x exceeds ~0.10. The insensitivity of ϕ_r to potential with 514.5 nm excitation is a case in point (Fig. 2 and 5). We circumvented this problem in one instance by exploiting the negative temperature dependence of the CdS:Te band gap. Sufficiently large values of ϕ_x were obtained with 514.5 nm excitation at elevated temperatures to yield ϕ_{r_o}/ϕ_r values well in excess of unity.[21] A method not requiring a change in PEC parameters is differential luminescence which was used to detect quenching by charge transfer in p-GaP when ϕ_x was only ~0.01.[1]

A strategy employing PTS to correlate temperature changes with ϕ_x has recently been described.[16,18] This technique permits the simultaneous determination of ϕ_x and energy efficiency without a calibrated light source. It also provides a method for independently monitoring ϕ_{nr} and should be useful for examining our assumptions regarding the potential dependence of ϕ_r and ϕ_{nr}.

A key question related to our studies of excited-state decay routes in CdS:Te-based PECs is their applicability to other systems. It is gratifying to see that similar relationships between ϕ_x and ϕ_r obtain for both 100 and 1000 ppm CdS:Te in aqueous sulfide electrolyte. The excited-state manifolds of these species differ considerably: Lightly doped samples such as 100 ppm CdS:Te are believed to have states ~0.2 eV above the valence band edge; in addition to these states, more heavily doped samples such as 1000 ppm CdS:Te have states ~0.4-0.6 eV above the valence band edge.[10-12] Interestingly, both samples also exhibit an emission band at ~505 nm, near the band gap edge; this transition is observable in electroluminescence and photoluminescence experiments under certain conditions.[24] It is quenched by photocurrent roughly in parallel with the lower energy emission band.

Besides CdS:Te, n-type ZnO, ZnO:Cu and p-type GaP have been examined with respect to relationships between photocurrent and emission intensity. Whereas CdS:Te electrochemistry consisted of oxidation of an electrolyte reductant, ZnO underwent photoanodic decomposition (to Zn^{2+} and O_2) and p-GaP gave reduction of water in the electrolytes employed.[1,2] A rigorous treatment of photocurrent and emission intensity in terms of absorptivity, depletion region width, surface properties, carrier density, lifetime, and diffusion length was presented in these studies. At least in the limiting cases of low and high ϕ_x, the potential dependence of ϕ_r was consistent with our results: besides the small dependence described above for p-GaP, no potential dependence of ϕ_r was observed in the ZnO system with band gap edge excitation; on the other hand, complete extinction of emission could be obtained with ultraband gap excitation at positive potentials, consistent with a ϕ_x value near unity (Table I). A mirror-symmetry in the iLV curve, predicted from both eq. 4 and a derivation presented in the ZnO study, was approximated by some of the ZnO experimental data.

The foregoing observations indicate that there may, indeed, be general correlations among ϕ_x, ϕ_r, and ϕ_{nr}. Incorporation of other data (absorptivity, carrier properties, etc.), examination of other systems, and the use of an independent probe for ϕ_{nr} such as PTS, should enable us to construct a refined model for excited-state decay processes of PECs.

We are grateful to the Office of Naval Research for support of this work. We also thank Professor Allen J. Bard for a preprint of ref. 18 and stimulating discussions.

1 K. H. Beckmann and R. Memming, J. Electrochem. Soc., 1969, 116, 368.

2 G. Petermann, H. Tributsch, and R. Bogomolni, J. Chem. Phys., 1972, 57, 1026.

3 B. Pettinger, H.-R. Schöppel, and H. Gerischer, Ber. Bunsenges. Phys. Chem., 1976, 80, 849.

4 D. J. Benard and P. Handler, Surf. Sci., 1973, 40, 141.

5 A. B. Ellis and B. R. Karas, J. Amer. Chem. Soc., 1979, 101, 236.

6 A. B. Ellis and B. R. Karas, Adv. Chem. Ser., 1980, 184, 185.

7 B. R. Karas and A. B. Ellis, J. Amer. Chem. Soc., 1980, 102, 968.

8 D. Dutton, Phys. Rev., 1958, 112, 785.

9 A. C. Aten, J. H. Haanstra, and H. deVries, Philips. Res. Reports, 1965, 20, 395.

10 J. D. Cuthbert and D. G. Thomas, J. Appl. Phys. 1968, 39, 1573.

11 D. M. Roessler, J. Appl. Phys., 1970, 41, 4589

12 P. F. Moulton, Ph.D. Dissertation, Massachusetts Institute of Technology, 1975.

13 A. B. Ellis, S. W. Kaiser, and M. S. Wrighton, J. Amer. Chem. Soc., 1976, 98, 6855.

14 H. Gerischer, J. Electroanal. Chem., 1975, 58, 263.

15 L. R. Faulkner and A. J. Bard, Electroanalytical Chemistry, ed. A. J. Bard (Marcel Dekker, Inc., New York, 1977), vol. 10, chap. 1, p. 1.

16 A. Fujishima, G. H. Brilmyer, and A. J. Bard, Semiconductor Liquid-Junction Solar Cells, ed., A. Heller (The Electrochemical Society Softbound Proceedings Series, Princeton, N.J., 1977), p. 172.

17 G. H. Brilmyer, A. Fujishima, K. S. V. Santhanam, and A. J. Bard, Anal. Chem., 1977, 49, 2057.

18 A. Fujishima, Y. Maeda, K. Honda, G. H. Brilmyer, and A. J. Bard, J. Electrochem. Soc., 1980, 127, 840.

19 A. Fujishima, H. Masuda, K. Honda, and A. J. Bard, Anal. Chem., 1980, 52, 682.

20 G. H. Brilmyer and A. J. Bard, Anal. Chem., 1980, 52, 685.

21 B. R. Karas, D. J. Morano, D. K. Bilich, and A. B. Ellis, J. Electrochem. Soc., 1980, 127, in press.

22 N. J. Turro, Modern Molecular Photochemistry (Benjamin/Cummings Publishing Co., Inc., Menlo Park, Calif., 1978), chap. 8, p. 232 and references therein.

23 D. F. Blossey and P. Handler, Semiconductors and Semimetals, ed., R. K. Willardson and A. C. Beer (Academic Press, New York, 1972), vol. 9, chap. 3, p. 257.

24 D. J. Morano, B. R. Karas, H. H. Streckert, and A. B. Ellis, submitted for publication.

TABLE 1. RELATIONSHIP BETWEEN ϕ_x AND ϕ_{r_o}/ϕ_r [a]

ϕ_x	ϕ_{r_o}/ϕ_r
0.001	1.00
0.01	1.01
0.05	1.05
0.10	1.11
0.20	1.25
0.30	1.43
0.40	1.67
0.50	2.00
0.60	2.50
0.70	3.33
0.80	5.00
0.90	10.00
1.00	∞

[a]Calculated from eq. 4 where ϕ_x is the photocurrent quantum yield, and ϕ_{r_o}/ϕ_r is the ratio of emission quantum yields between open circuit and the potential where ϕ_x is measured.

TABLE 2. COMPARISON BETWEEN MEASURED AND CALCULATED VALUES OF ϕ_x

Electrode (Fig.)[a]	Excitation λ/nm[b]	ϕ_x, meas.[c]	ϕ_x, calc.[d]
100 ppm CdS:Te(2)	514.5	0.07	0.00
(3)	488.0	0.49	0.64
(4)	P	0.28	0.04
(4)	P	0.28	0.31[e]
1000 ppm CdS:Te (5)	514.5	0.12	0.04
(6)	488.0	0.74	0.66
(7)	P	0.60	0.31
(7)	P	0.60	0.56[e]

[a]The indicated electrode was used in the PEC shown in Fig. 1. Table entries are based on experimental results in the indicated figures.

[b]Excitation wavelength. An entry of P denotes polychromatic laser excitation with compositions given in the Fig. 4 and 7 captions.

[c]Photocurrent quantum efficiency measured at -0.3 V vs. SCE by the procedure described in the Experimental Section. Entries are estimated to be accurate to ±5%, uncorrected for reflective losses and electrolyte absorption.

[d]Photocurrent quantum efficiency calculated at -0.3 V vs. SCE with eq. 4 from the observed ratio of open-circuit emission intensity to the emission intensity at -0.3 V vs. SCE. The midpoints of the emission intensity error bars were used for these calculations. We estimate that values are accurate to ±15% based on the full error bars.

TABLE 2. continued

[e]Photocurrent quantum efficiency calculated at -0.3 V vs. SCE using a weighted average of the measured ϕ_x values for the individual monochromatic laser excitation lines which make up the polychromatic excitation. For Fig. 4 the composition is roughly 44% 514.5 nm and 56% ultraband gap excitation; for Fig. 7, 29% 514.5 nm and 71% ultraband gap excitation. The 488.0 nm ϕ_x value was used in each case as representative of the ultraband gap wavelengths.

Fig. 1.- Top view of the experimental arrangement used for observing front-surface emission from a CdS:Te photoelectrode: A, laser; B, monochromator; C, beam expander followed by slit; D, emissive CdS:Te photoelectrode, the site of S^{2-} oxidation (not pictured are a Pt counterelectrode at which H_2 evolution occurs, a SCE, and a potentiostat/programmer to which all three electrodes are connected); E, aqueous, N_2-purged, sulfide (1M OH^-/1 M S^{2-}) electrolyte; F, emission detection optics.

Fig. 2. - Photocurrent (bottom frame) and emission intensity (top frame) monitored at 600 nm vs. potential for a 100 ppm CdS:Te single-crystal electrode in sulfide electrolyte. The ~0.18 cm^2 exposed electrode area was excited with 0.11 mW at 514.5 nm. The error bars for each measurement are plotted and are primarily due to laser intensity fluctuations. Open circles in the top frame represent the calculated emission intensity (see text); the open circuit calculated value has been arbitrarily set at the midpoint of the observed emission intensity error bar. Midpoints of the photocurrent error bars have been used for the emission intensity calculation at the other potentials shown.

Fig. 3 - Photocurrent (bottom frame) and emission intensity (top frame) monitored at 600 nm vs. potential for 488.0 nm excitation (0.14 mW) of the PEC of Fig. 2. Because the geometry is unchanged from Fig. 2, the emission intensity and photocurrent from the two excitation wavelengths may be directly compared when corrected to matching incident intensities (ein/sec). The error bars and open circles (top frame) have the same meaning as in Fig. 2.

Fig. 4. - Photocurrent (bottom frame) and emission intensity (top frame) monitored at 600 nm vs potential for polychromatic excitation (0.20 mW) of the PEC of Fig. 2 and 3. The polychromatic light consists principally of 514.5 nm (44% by power), 496.5 nm (16%), 488.0 nm (32%), and 476.5 nm (8%). The PEC geometry is unchanged from Fig. 2 and 3. Error bars represent the range of measured values. Open circles in the top frame stand for emission intensities calculated by treating the exciting light as monochromatic; triangles are values calculated from a weighted average of the emission intensities obtained for the constituent monochromatic wavelengths (see text). The weighted average at open circuit, when corrected for the increased incident intensity used in this experiment, is ~20% above the midpoint of the observed emission intensity and has been arbitrarily scaled down to match this value; the emission intensities calculated in this manner at the other potentials were then also scaled down by this same factor.

Fig. 5. - Photocurrent (bottom frame) and emission intensity (top frame) monitored at 670 nm vs potential for a 1000 ppm CdS:Te single-crystal electrode in sulfide electrolyte. The ~0.18 cm^2 exposed electrode area was excited with 0.040 mW at 514.5 nm. Error bars for each measurement are shown. Open circles are calculated emission intensities as described in the text and in Fig. 2.

Fig. 6. - Photocurrent (bottom frame) and emission intensity (top frame) monitored at 670 nm vs. potential for 488.0 nm excitation (0.038 mW) of the PEC of Fig. 5. The geometry is unchanged from Fig. 5 so that emission intensity and photocurrent from the two excitation wavelengths may be directly compared when corrected to matching incident intensities (ein/sec). Error bars and open circles have the same meaning as in Fig. 2.

Fig. 7.- Photocurrent (bottom frame) and emission intensity (top frame) monitored at 670 nm vs. potential for polychromatic excitation (0.047 mW) of the PEC of Fig. 5 and 6. Composition of the polychromatic light is principally 514.5 nm (29% by power), 496.5 nm (19%), 488.0 nm (37%), and 476.5 nm (14%). The PEC geometry is invariant with respect to Fig. 5 and 6. Error bars, open circles and triangles have the same significance as in Fig. 4. The actual weighted average at open circuit, when corrected for incident intensity variations in Fig. 5-7, is ~30% below the midpoint of the observed emission intensity and has been scaled up to match this value; the emission intensities calculated in this manner at the other potentials were then also scaled up by this same factor.

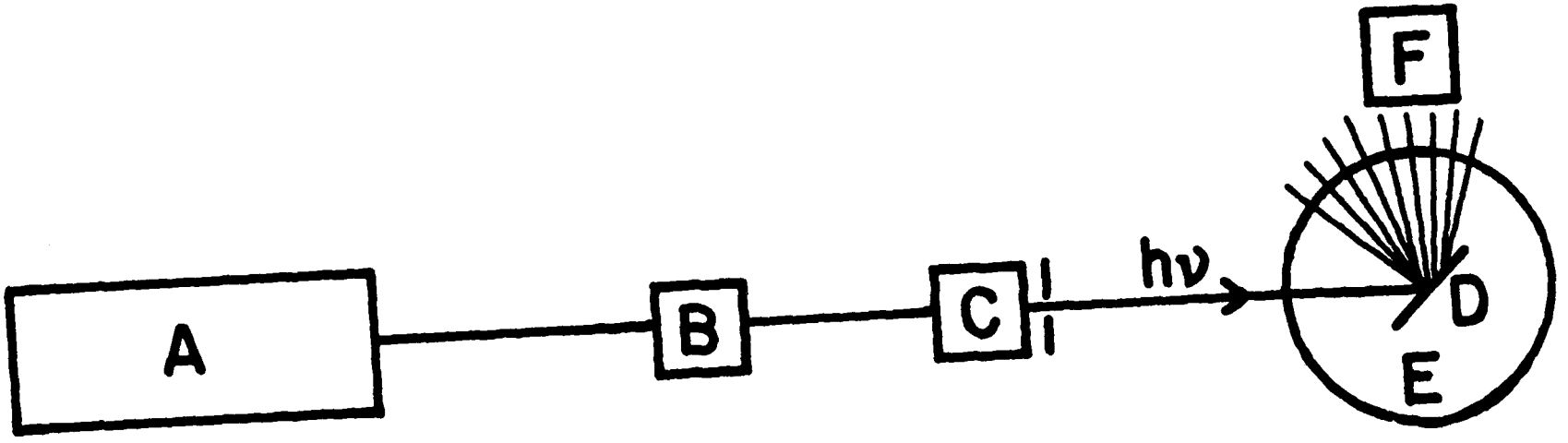
A
B
C
hν
F
D
E

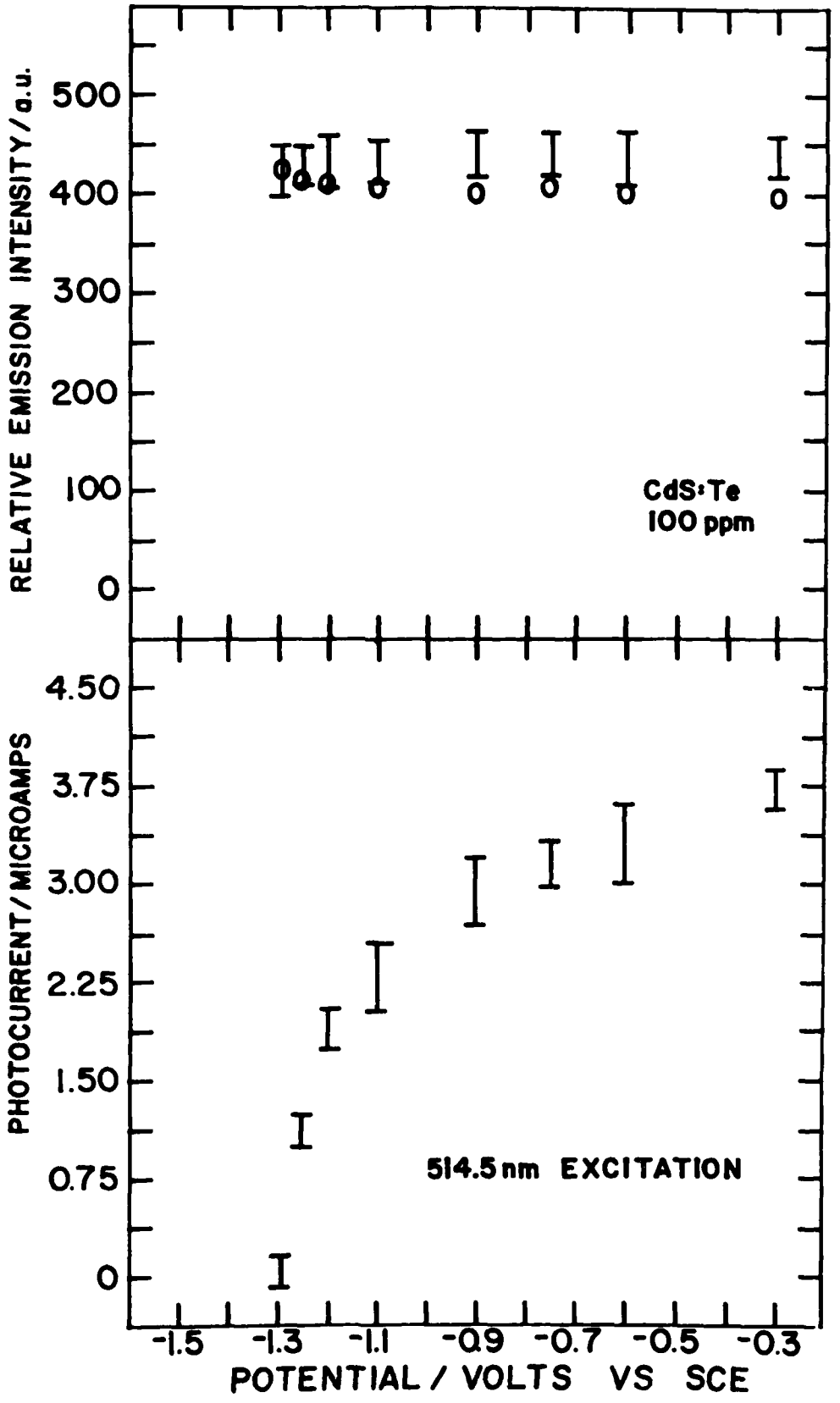
RELATIVE EMISSION INTENSITY/a.u.
500
400
300
200
100
0
CdS:Te
100 ppm
PHOTOCURRENT/MICROAMPS
4.50
3.75
3.00
2.25
1.50
0.75
0
514.5nm EXCITATION
-1.5
-1.3
-1.1
-0.9
-0.7
-0.5
-0.3
POTENTIAL / VOLTS VS SCE

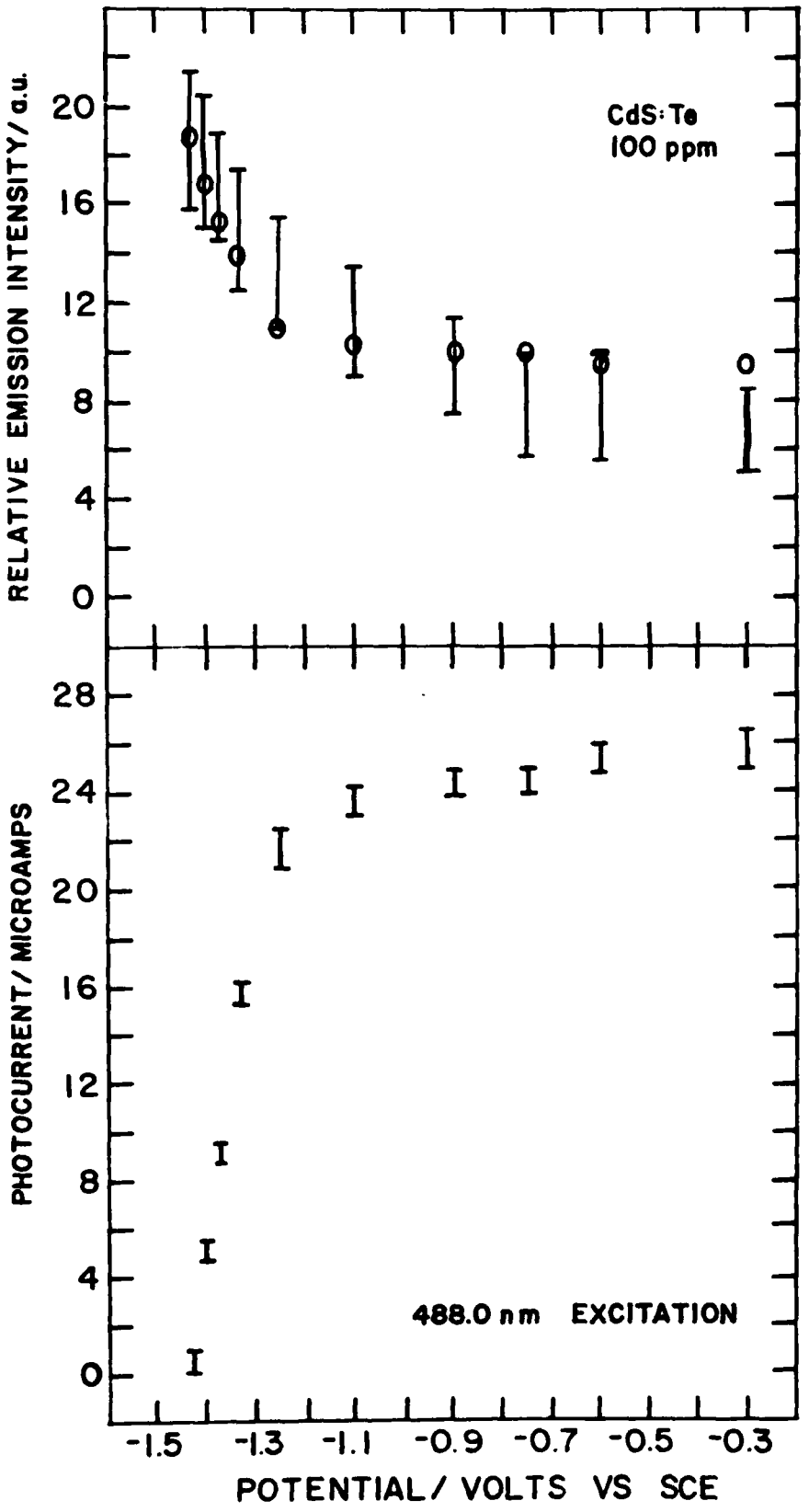
RELATIVE EMISSION INTENSITY/ a.u.
20
16
12
8
4
0
CdS:Te
100 ppm
PHOTOCURRENT/ MICROAMPS
28
24
20
16
12
8
4
0
488.0 nm EXCITATION
-1.5
-1.3
-1.1
-0.9
-0.7
-0.5
-0.3
POTENTIAL/ VOLTS VS SCE

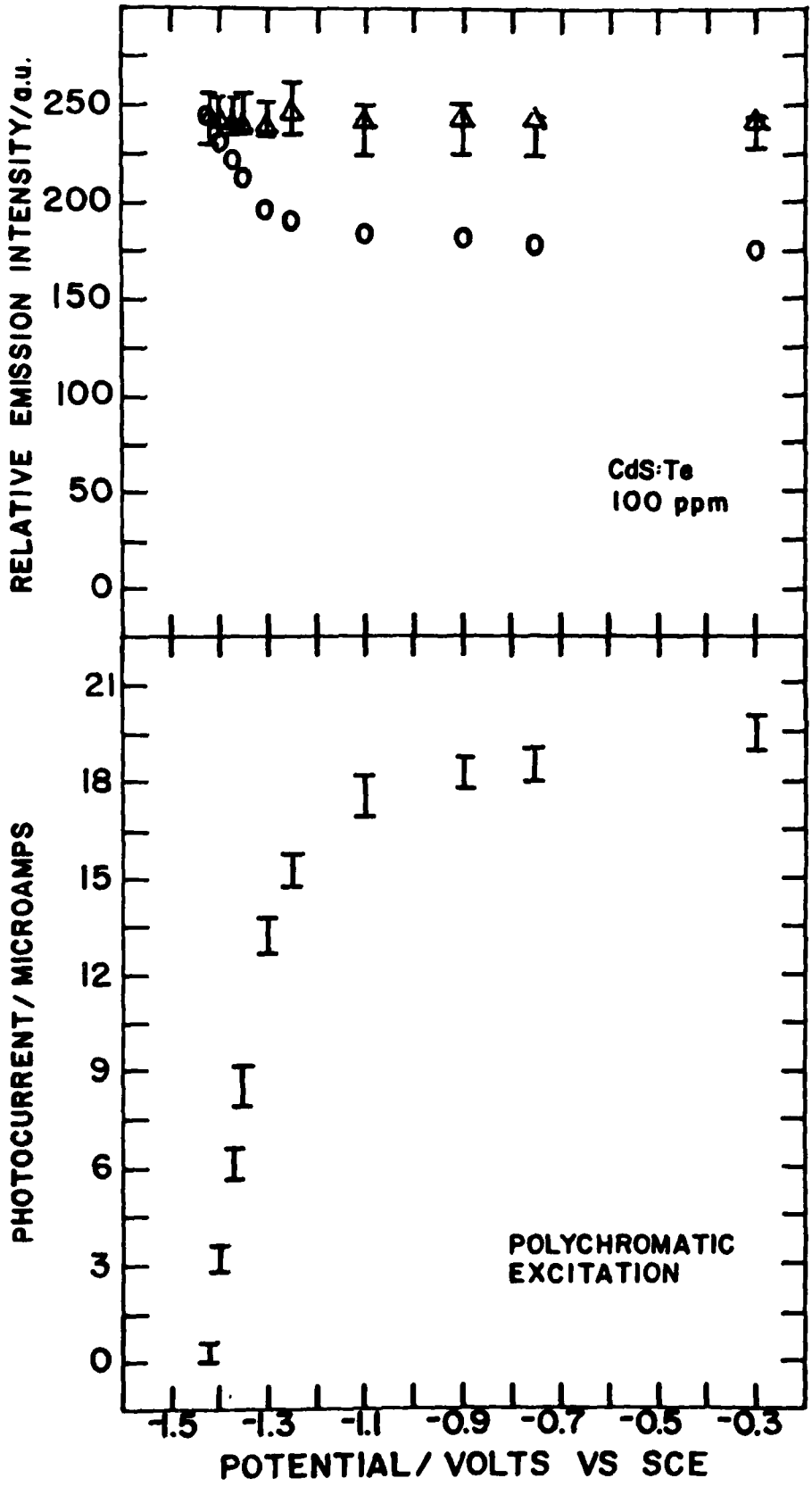
RELATIVE EMISSION INTENSITY/a.u.
250
200
150
100
50
0
CdS:Te
100 ppm
PHOTOCURRENT/ MICROAMPS
21
18
15
12
9
6
3
0
POLYCHROMATIC
EXCITATION
-1.5
-1.3
-1.1
-0.9
-0.7
-0.5
-0.3
POTENTIAL/ VOLTS VS SCE

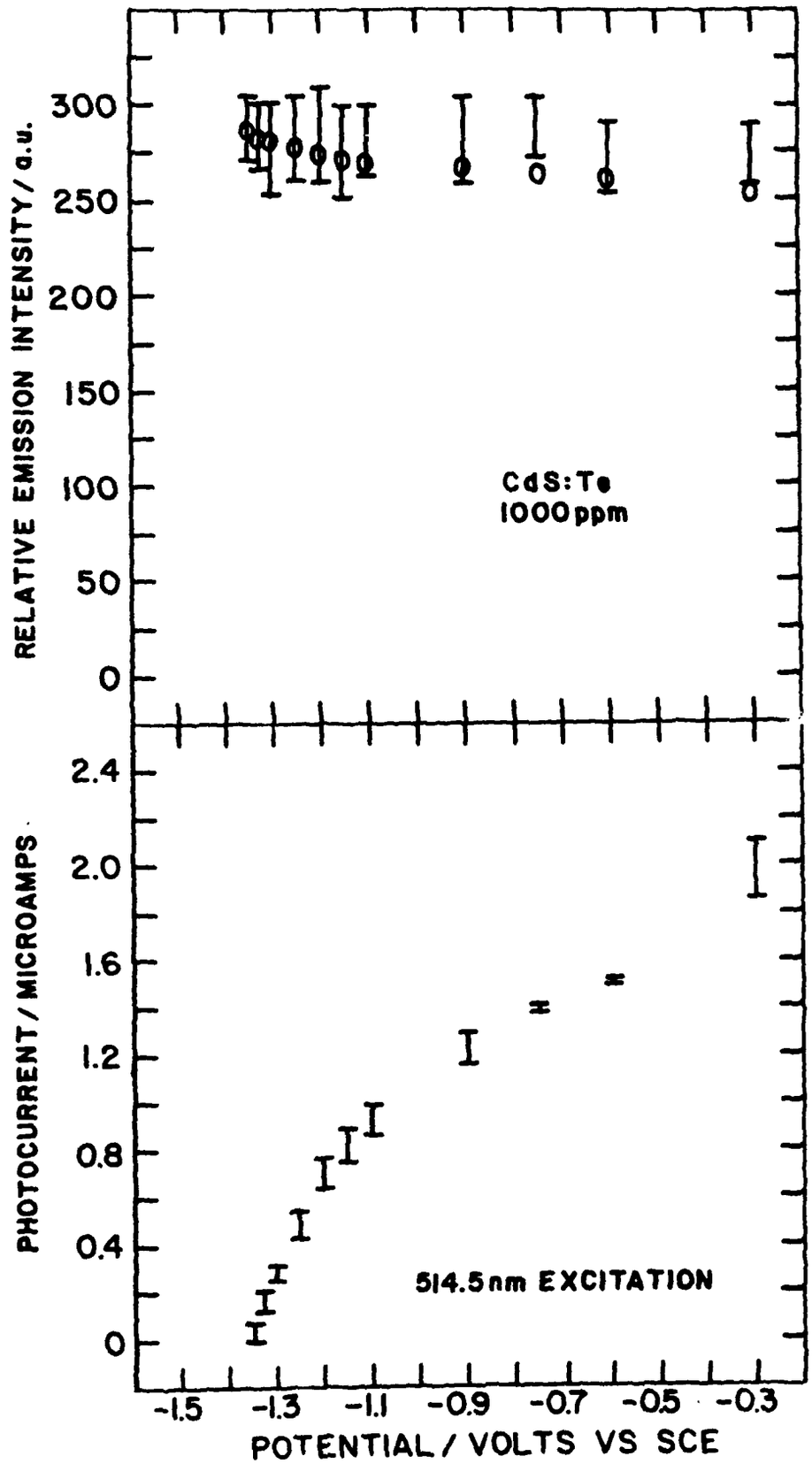
RELATIVE EMISSION INTENSITY / a.u.
300
250
200
150
100
50
0
CdS:Te
1000ppm
PHOTOCURRENT / MICROAMPS
2.4
2.0
1.6
1.2
0.8
0.4
0
514.5nm EXCITATION
-1.5
-1.3
-1.1
-0.9
-0.7
-0.5
-0.3
POTENTIAL / VOLTS VS SCE

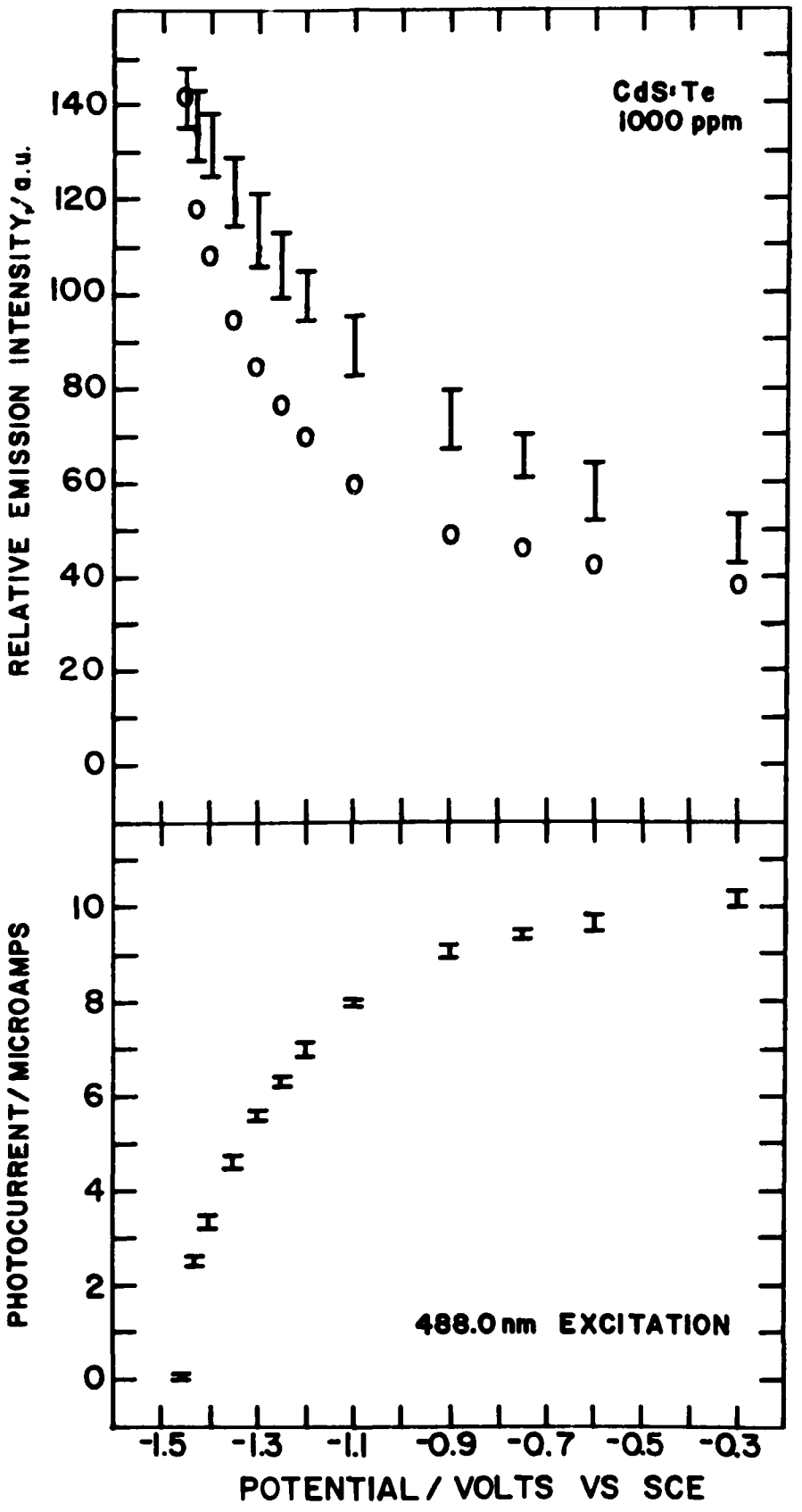
CdS:Te
1000 ppm
RELATIVE EMISSION INTENSITY/a.u.
140
120
100
80
60
40
20
0
PHOTOCURRENT/MICROAMPS
10
8
6
4
2
0
488.0nm EXCITATION
-1.5
-1.3
-1.1
-0.9
-0.7
-0.5
-0.3
POTENTIAL/VOLTS VS SCE

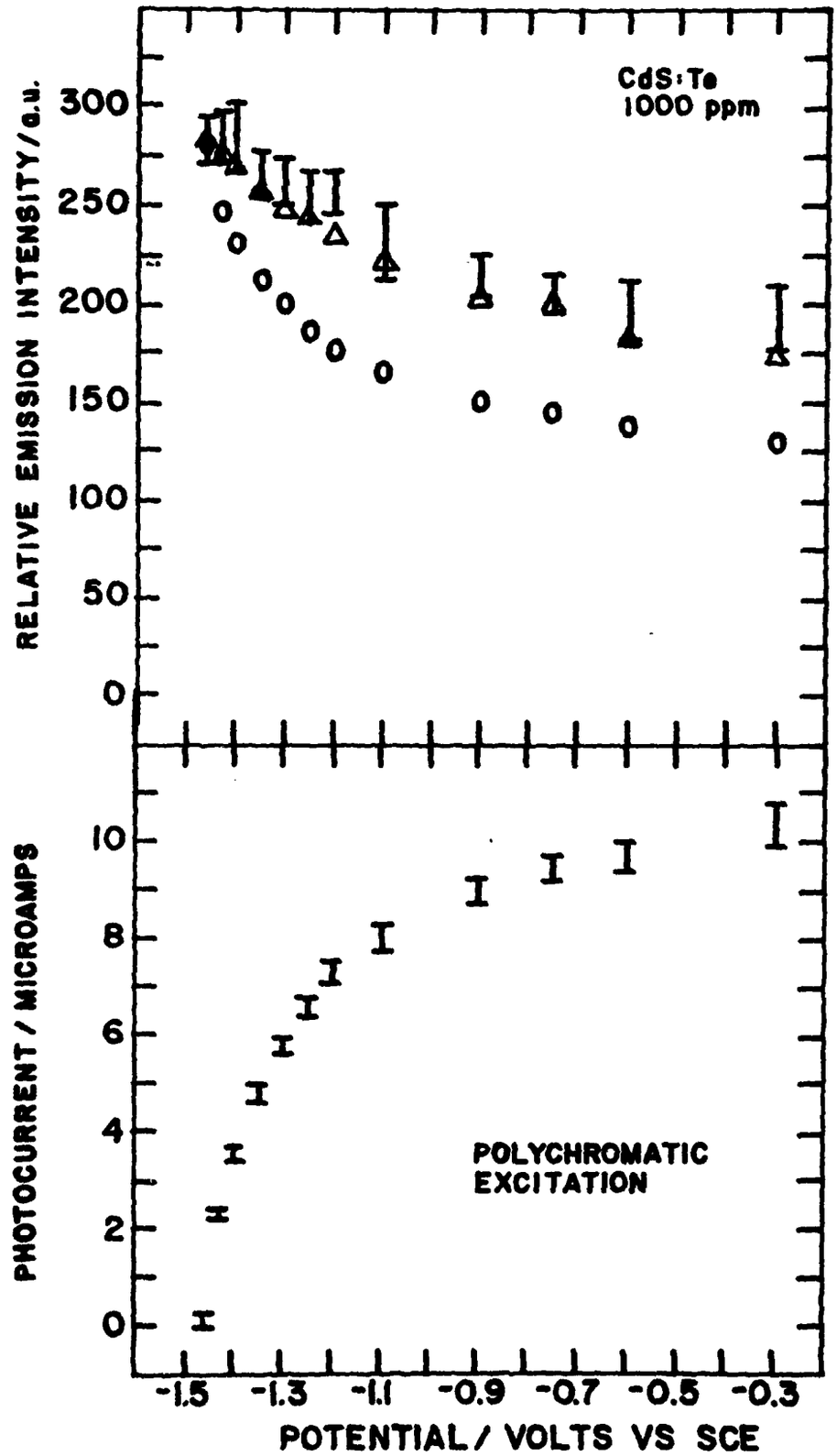
CdS:Te
1000 ppm
RELATIVE EMISSION INTENSITY/a.u.
300
250
200
150
100
50
0
PHOTOCURRENT / MICROAMPS
10
8
6
4
2
0
POLYCHROMATIC
EXCITATION
-1.5
-1.3
-1.1
-0.9
-0.7
-0.5
-0.3
POTENTIAL / VOLTS VS SCE